

## *Supplement of*

## **Variable effects of spatial resolution on modeling of nitrogen oxides**

Chi Li<sup>1</sup>, Randall V. Martin<sup>1</sup>, Ronald C. Cohen<sup>2,3</sup>, Liam Bindle<sup>1</sup>, Dandan Zhang<sup>1</sup>, Deepangsu Chatterjee<sup>1</sup>, Hongjian Weng<sup>4</sup>, and Jintai Lin<sup>4</sup>

<sup>1</sup>Department of Energy, Environmental Chemical Engineering, Washington University in St. Louis, St. Louis, MO, USA

<sup>2</sup>Department of Chemistry, University of California, Berkeley, Berkeley, CA, USA

<sup>3</sup>Department of Earth and Planetary Science, University of California, Berkeley, Berkeley, CA, USA

<sup>4</sup>Laboratory for Climate and Ocean-Atmosphere Studies, Department of Atmospheric and Oceanic Sciences, School of Physics, Peking University, Beijing, China

**Correspondence:** Chi Li (lynchlee90@gmail.com)

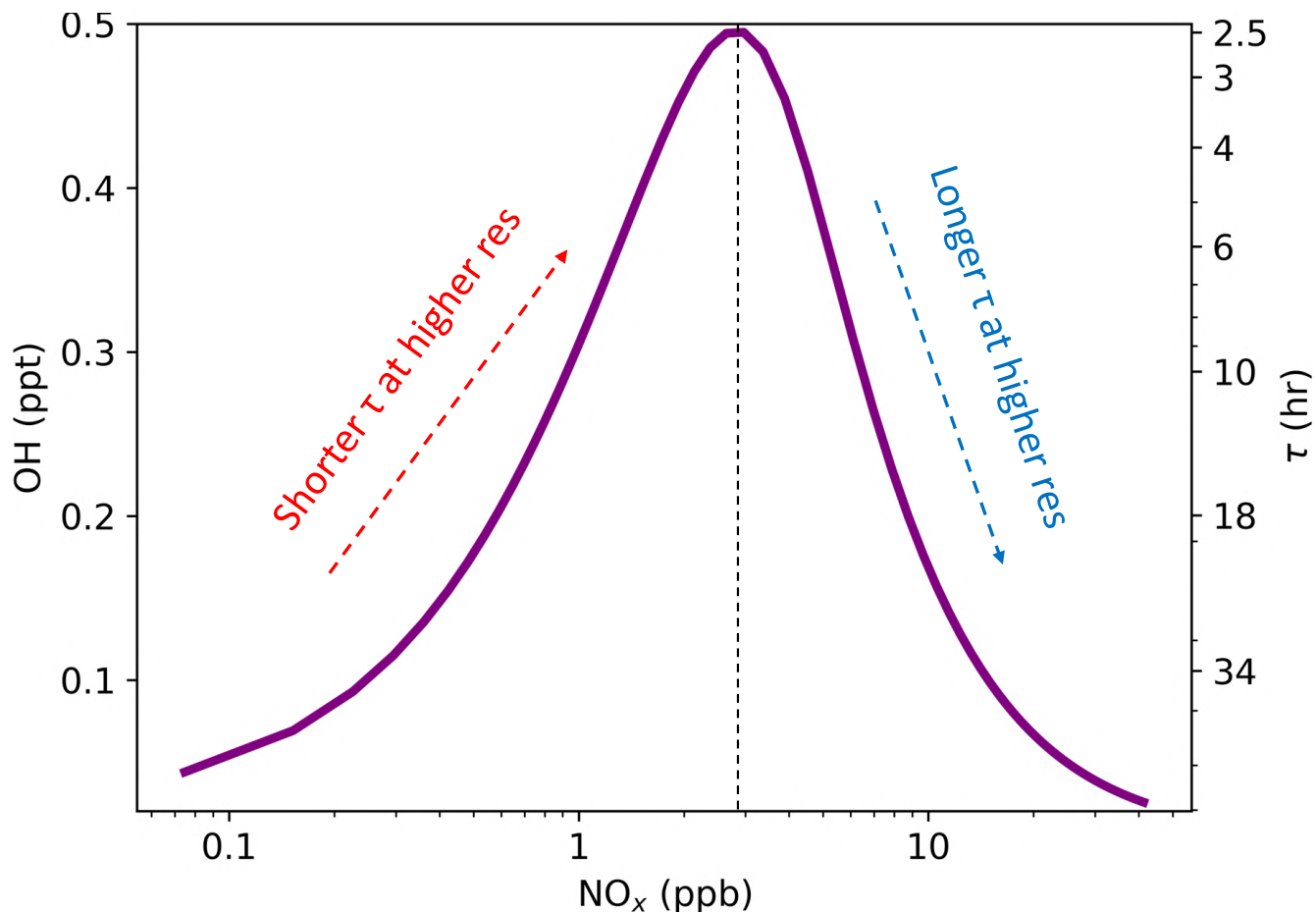


**Figure S1.** Illustration of the daytime  $\text{NO}_x$ -OH-lifetime feedback. Higher resolution modeling tends to concentrate the most  $\text{NO}_x$  emissions near sources, thus will decrease  $\text{NO}_x$  lifetime in the  $\text{NO}_x$ -limited regime (left) and increase  $\text{NO}_x$  lifetime in the  $\text{NO}_x$ -saturated regime (right). The steady-state concentrations were calculated assuming a  $\text{NO}_2/\text{NO}$  ratio of 4, an alkyl nitrate branching ratio of 0.04, a VOC reactivity of  $3 \text{ s}^{-1}$ , an initial ozone concentration of 25 ppb, and the production of  $\text{HO}_x$  is proportional to ozone.

Surface  $\text{NO}_x$  mixing ratio at 13 km and biases at the other resolutions

(a) July, UTC 15-18

(b) July, UTC 21-24

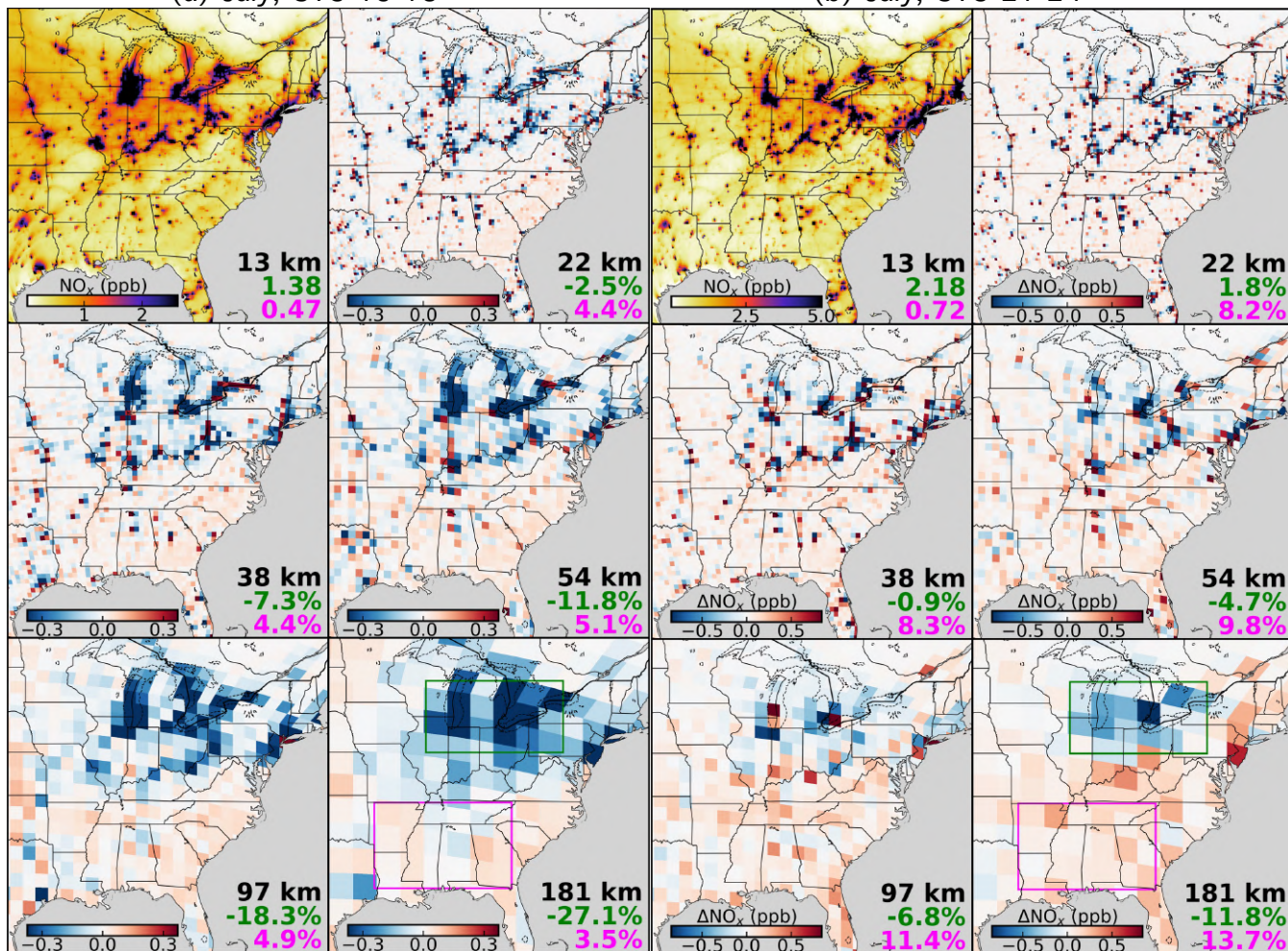


**Figure S2.** Similar to Figure 1c but for morning (a. UTC 15-18 or CST 9-12) and afternoon (b. UTC 21-24 or CST 15-18), respectively.

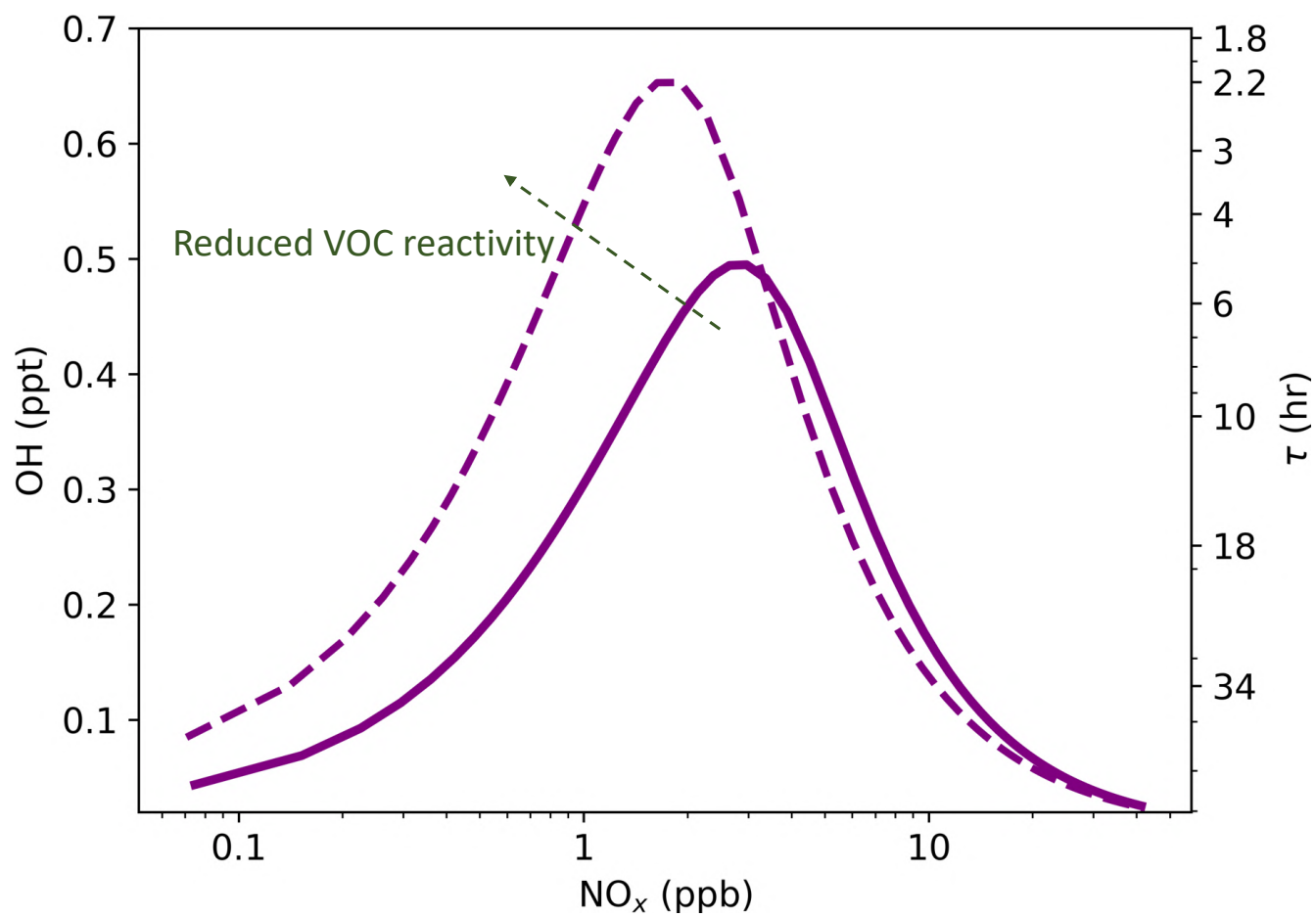


**Figure S3.** As in Figure S1 but including an additional scenario where the VOC reactivity is reduced by 50% (dashed).

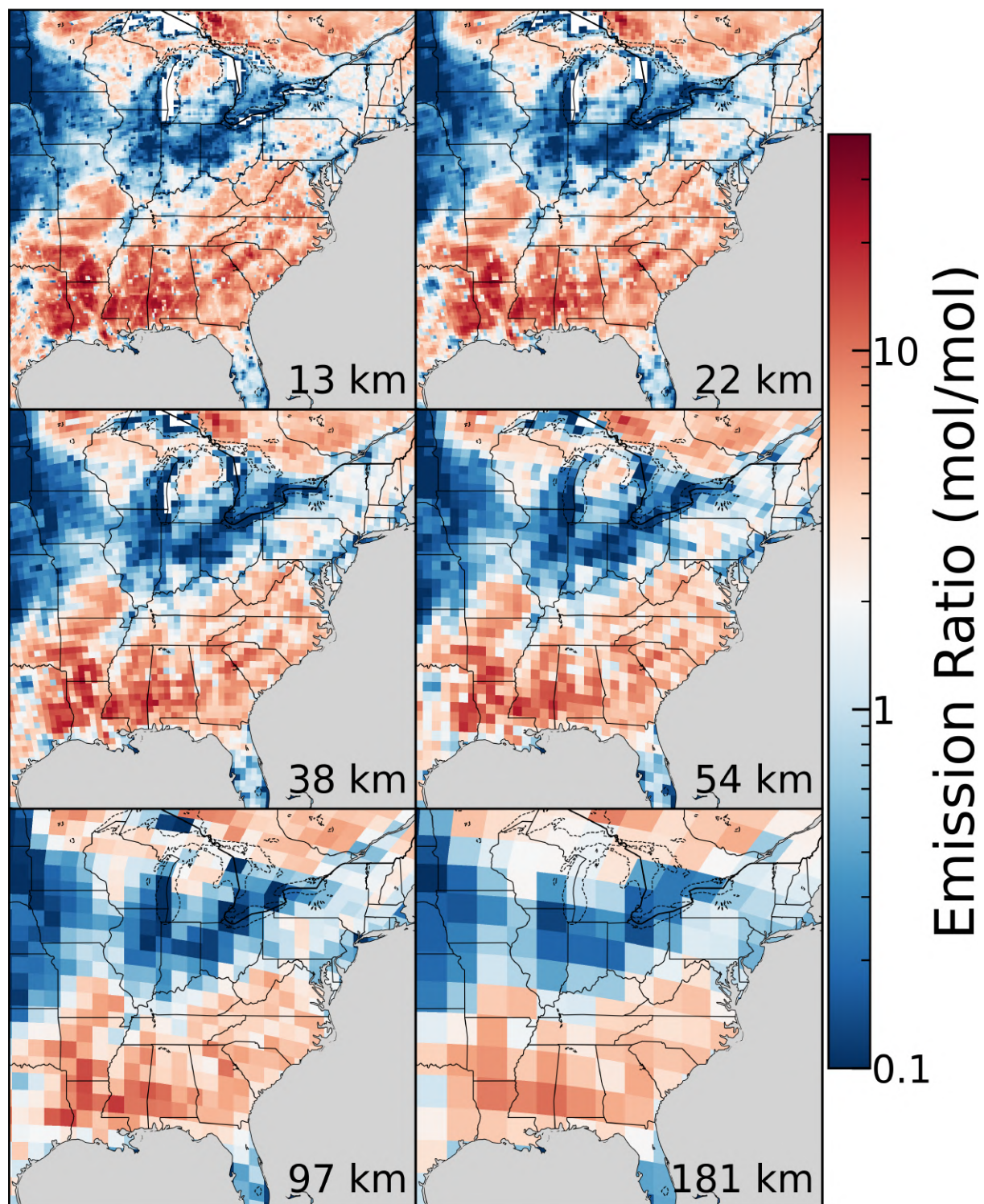


**Figure S4.** Similar to Figure 1a but including all the six resolutions.

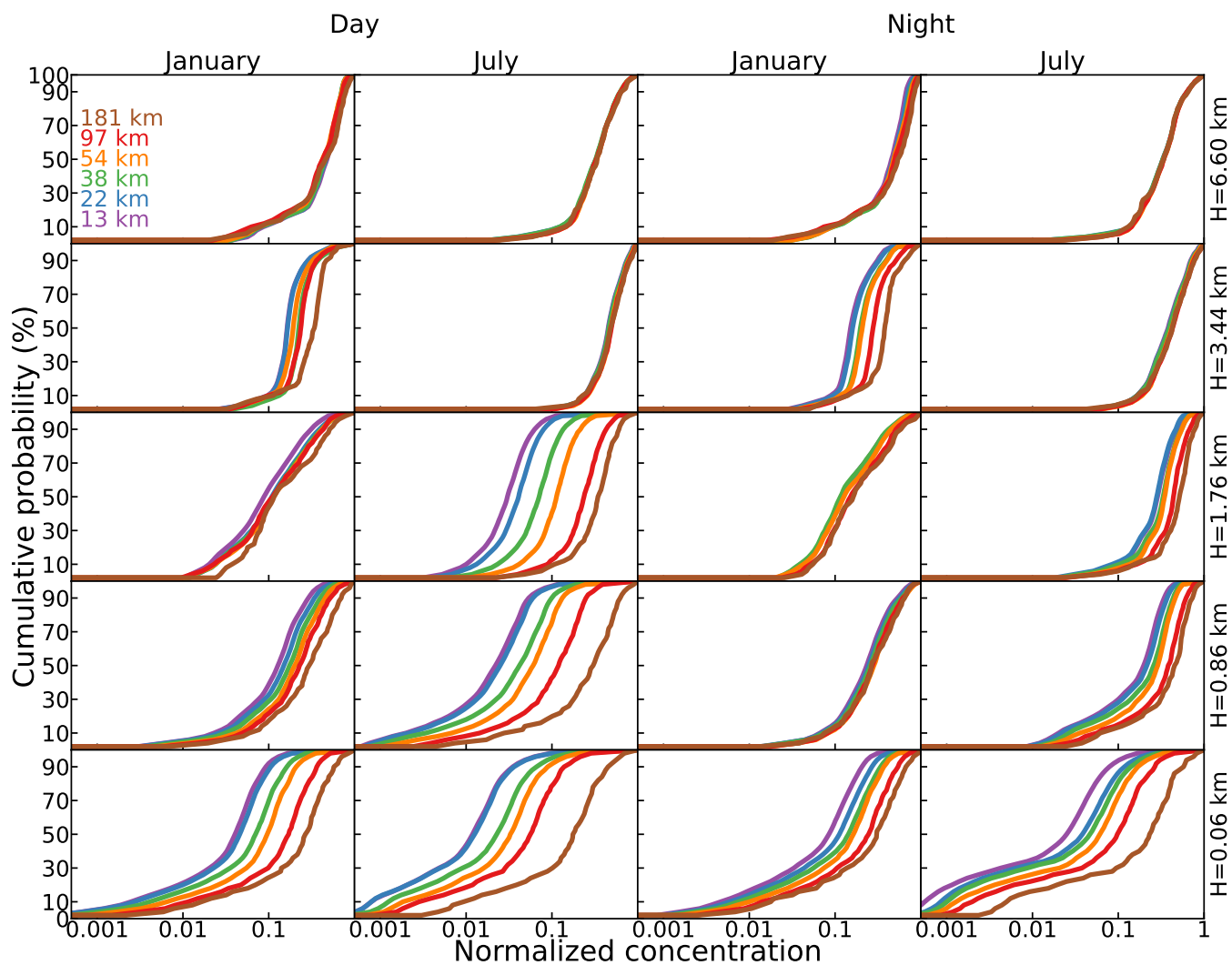


**Figure S5.** Cumulative histogram of simulated  $\text{NO}_x$  concentration (normalized to 0-1) at different altitudes (rows, each corresponding to the 1st, 7th, 13th, 19th and 25th layer of GEOS-Chem) and resolutions (colors) within the eastern US domain. The  $\text{NO}_x$  spatial heterogeneity is reduced at coarser vs. finer resolutions, at colder vs. warmer seasons, at higher vs. lower altitudes, and at nighttime vs. daytime.

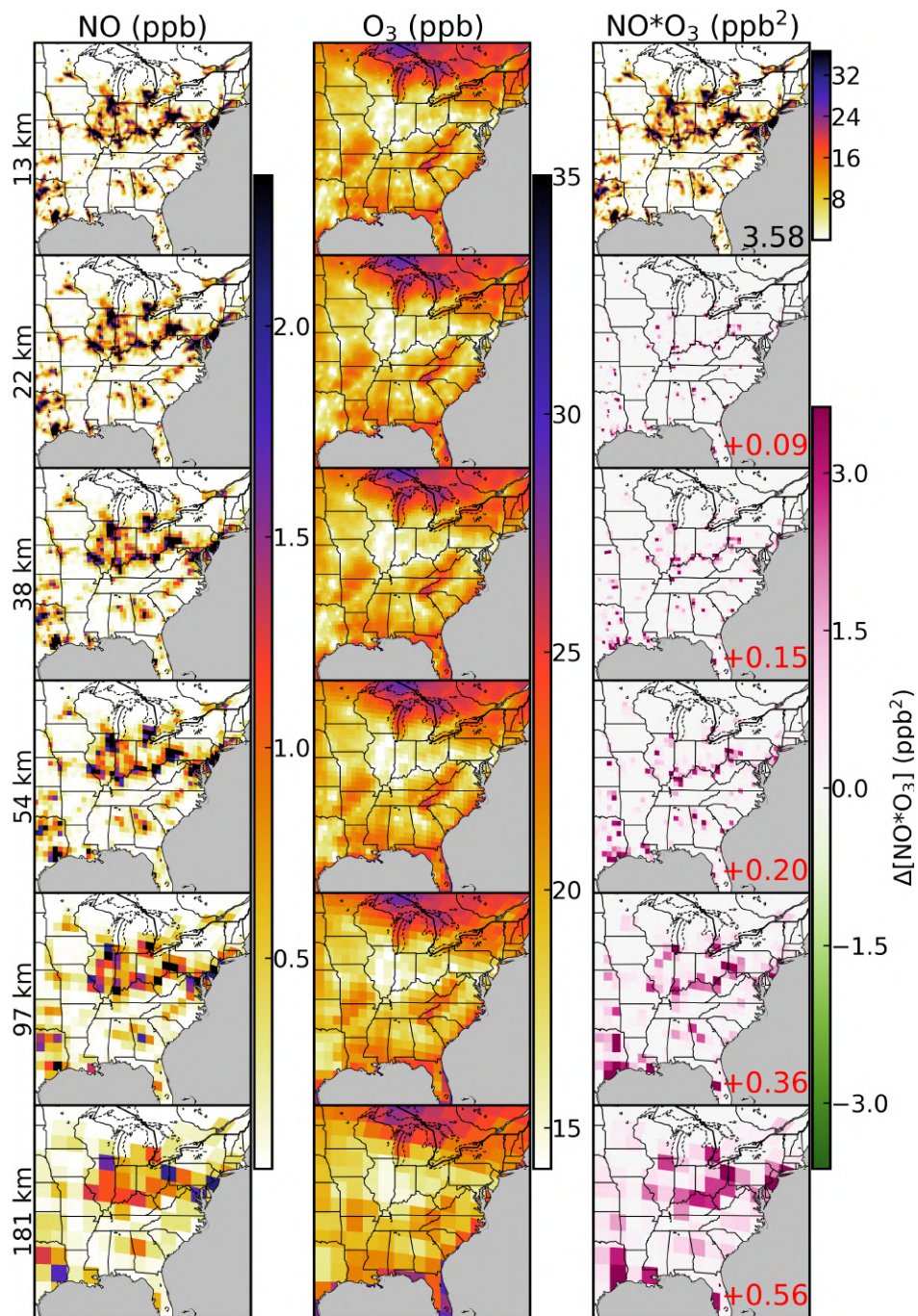


**Figure S6.** Illustration of the resolution-dependent nighttime NO-O<sub>3</sub> titration efficiency. Left and middle panels are mean surface NO and O<sub>3</sub> concentration at UTC+6 in January 2015, at 13 km (uppermost panels) and regridded to the other resolutions. The rightmost panels show their products at 13 km resolution, and differences if calculated at the other coarser resolutions. Domain-mean products and differences are inset.



# Tropospheric NO<sub>2</sub> slant column density at 13 km and biases at the other resolutions

(a) January

(b) July

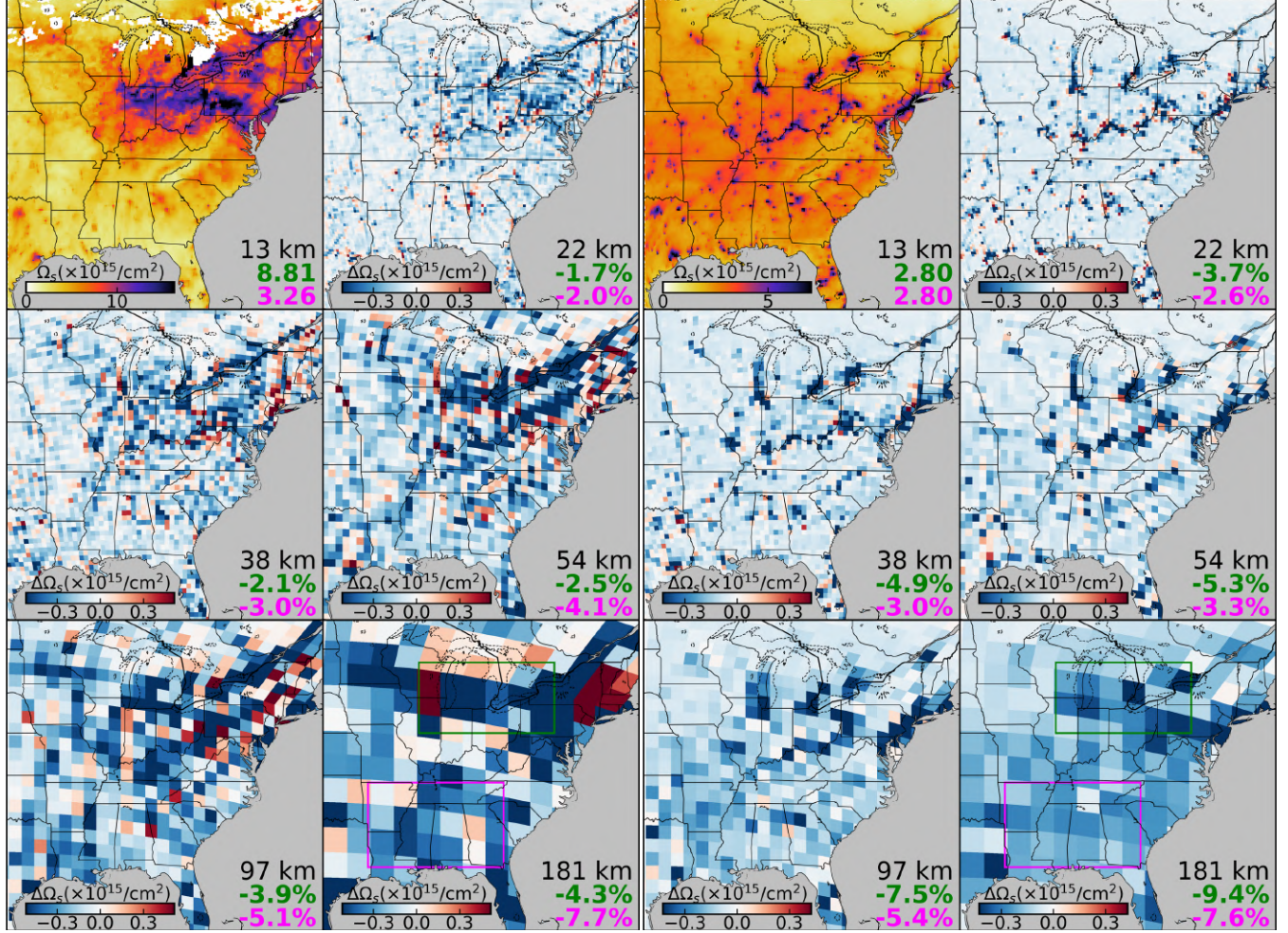


**Figure S8.** Similar to Figure 7 but for slant column density ( $\Omega_s$ , molecules/cm<sup>2</sup>) calculated from GEOS-Chem NO<sub>2</sub> mixing ratios and scattering weights corresponding to TROPOMI observations. The small blank (white) areas in January have no available TROPOMI retrievals under clear sky and snow-free conditions.